

# Evaluation of Ventricular Function with First-Pass Iridium-191m Radionuclide Angiocardiology

Chaim Hellman, Nili Zafir, Aharon Shimoni, David Issachar, Jacob Trumper, Shmuel Abrashkin, and Ernesto Lubin

*The Massada Nuclear Cardiology Unit, Division of Nuclear Medicine, Beilinson Medical Center, Petach Tikva, Israel and the Radiopharmaceutical Research Unit, Nachal Soreq Nuclear Research Center, Nachal Soreq, Israel*

Iridium-191m would appear to be a highly useful agent for first-pass radionuclide angiocardiology (FPNA), with its very short half-life (4.96 sec), dual photopeaks (65 and 129 keV), and high injectable activity levels ( $>100$  mc). In order to compare  $^{191m}\text{Ir}$  FPNA to current methods used to define cardiac function, 20 patients referred for cardiac catheterization were studied. Count rate data, right ventricular (RV), and left ventricular ejection fraction (LVEF), LV and diastolic volume (EDV), and end diastolic long axis (AXIS) were evaluated. Count rate data using  $^{191m}\text{Ir}$  FPNA was consistently better than similar data obtained by  $^{99m}\text{Tc}$  FPNA. There were acceptable correlations between  $^{191m}\text{Ir}$  and  $^{99m}\text{Tc}$  FPNA RVEF ( $r = 0.848$ ),  $^{191m}\text{Ir}$  FPNA and contrast angiography LVEF ( $r = 0.944$ ), LVEDV ( $r = 0.917$ ), and LV AXIS ( $r = 0.866$ ). The data thus suggests that  $^{191m}\text{Ir}$  FPNA has great potential in the evaluation of cardiac function.

J Nucl Med 30:450-457, 1989

First-pass radionuclide angiocardiology (FPNA) has been a well-documented means of assessing cardiac function (1-6) in addition to its ability to detect and assess congenital heart disease (7-12). Unfortunately, the radiopharmaceutical used most frequently, technetium-99m ( $^{99m}\text{Tc}$ ), has characteristics that are less than ideal for first-pass studies. Although its gamma energy is highly suitable (140 keV), its half-life of 6 hr is not ideal. Serial studies in adult patients, e.g., rest and exercise or multiple projections, are limited to one to three injections when using a dose of 15 to 20 mCi. A disturbingly high background may also be present in studies subsequent to the first dose. In addition, high efficiency collimators must be used to obtain a suitable count information density during acquisition; these collimators are accompanied by a lowered inherent spatial resolution.

Iridium-191m ( $^{191m}\text{Ir}$ ) has therefore been proposed as an alternative for first-pass studies by Treves et al. (13-15). Iridium-191m has the desirable physical characteristics of a very short half-life (4.9 sec) and dual peak

energy levels (65 and 129 keV) that can be easily imaged by a conventional high count rate gamma camera. These characteristics would allow larger doses of radioactivity with significantly lower radiation exposure to the patient, a near absent background in serial studies, and an end result of better counting statistics.

Unfortunately, generators of  $^{191m}\text{Ir}$  have not been clinically available, thus limiting the clinical evaluation of the radiopharmaceutical. Packard et al. has recently reported the development of a generator (16), that has been used to evaluate both children and adults (17) in preliminary studies. In this latter study by Heller et al., equipment not specifically designed for high count rates was employed, thus causing lower counting statistics and significant count losses (as high as 75%). This may negate some of the very potential benefits that are offered by using  $^{191m}\text{Ir}$ . Our laboratory also has had the opportunity to use a new  $^{191}\text{Os}/^{191m}\text{Ir}$  generator; it was developed by Soreq Nuclear Research Center and reported in an accompanying article (18).

The aim of this study was to assess the utility of  $^{191m}\text{Ir}$ , as obtained from the previously mentioned generator, in adult population FPNA using a high count-rate digital scintillation camera, and to compare the results to currently accepted examinations of cardiac

---

Received Feb. 19, 1988; revision accepted Dec. 9, 1988

For reprints contact: Chaim Hellman, MD, Div. of Nuclear Medicine, Beilinson Medical Center, Petach Tikva, Israel.

function in the cardiac catheterization and nuclear cardiology laboratories.

## METHODS

### Patient Population

Twenty patients formed the basis of this study. All patients were treated in compliance with the Helsinki Convention and signed informed consent. The patients had been referred to the nuclear cardiology unit for the evaluation of left ventricular function. Patient age ranged from 16 to 76 yr with a mean of 56 yr. Seventeen patients suffered from ischemic heart disease, two patients suffered from valvular heart disease (Patients 18 and 20), and one patient suffered from an anterior wall left ventricular (LV) myocardial infarction secondary to automobile accident trauma (Patient 8). With the exception of three patients, all other patients underwent cardiac catheterization, coronary arteriography, and LV contrast angiography performed within 72 hr of radionuclide angiocardigraphy. The remaining three patients (10, 17, and 20), also were studied by cardiac catheterization and contrast angiography, but in a period ranging from 15 to 32 days prior to radionuclide angiocardigraphy. All 20 patients had FPRA studies performed using both  $^{191\text{m}}\text{Ir}$  and  $^{99\text{m}}\text{Tc}$ . In 14 patients, multigated nuclear angiography (MUGA) was also performed.

### Contrast Angiography

All patients had selective coronary arteriography and contrast left ventriculography using Judkins technique from the right femoral artery (19). Contrast left ventriculography was performed in the 30-degree right anterior oblique (RAO) view using power injections of 24 ml to 40 ml of iodinated contrast material into the left ventricle in 2 to 3 sec. In all cases, cineangiograms were of good quality, allowing easy demarcation of the intracavitary borders. Calculations were made only on sinus rhythm beats.

The roentgenographic magnification factor was assessed by a 1.0-cm calibration marking on the tip of the left ventricular pigtail catheter. End diastolic and systolic areas and major axes as well as the magnification factor marking were traced on paper from a cineangiographic projector. To calculate area and length, a digitizer connected to an on-line computer was used. Left ventricular and diastolic volume (LVEDV) and left ventricular end systolic volume (LVESV) were then calculated by means of the Kasser-Kennedy RAO modification (20).

### Iridium-191m Generator

The generator used in this study was that developed and provided by the Soreq Nuclear Research Center and described in the accompanying paper to this study (18). It was part of a total system of delivery which included a new separation system for the  $^{191}\text{Os}/^{191\text{m}}\text{Ir}$  based on silica-gel impregnated with tridodecylmethylammonium chloride, a scavenger column packed with activated charcoal, and elution by pH 1 saline buffered by succinate or phosphate solutions prior to injection. The  $^{191\text{m}}\text{Ir}$  dosage given to patients was dependent on the date of the generator's preparation. A maximum of 150 mCi was administered shortly after generator availability to a minimum of 100 mCi given 14 days after availability. The injected  $^{191\text{m}}\text{Ir}$  activity was contained in 0.5 ml eluate and was followed by a 20-ml bolus of normal saline solution to

provide an adequate "push" of the radiotracer into the central circulation. In 18 patients, the dose was administered directly from the generator by manual means. In two patients, the dose, as well as the saline "push" was administered by a coordinated motor-driven infusion pump in an attempt to assure an accelerated, more uniform radiotracer delivery.

### Iridium-191m First-Pass Nuclear Angiocardigraphy Technique

Iridium-191m FPNA was performed using dual photopeak acquisition on an Elscint Apex 430 single crystal digital camera and dedicated computer system (Elscint, Ltd., Haifa, Israel). The two 20% windows were set over each of the 65-keV and 129-keV photopeaks. A source of directly eluted  $^{191\text{m}}\text{Ir}$  was used to determine the linearity of the scintillation camera system's counting statistics. It was found that above 320,000 cts/sec, significant loss (20%) occurred. Thus, a medium high efficiency 30-degree slant hole collimator [Elscint #16 Apex Collimator (APC-16)] was used as it was seen to provide the best counting statistics when 100-150 mCi of this radiotracer were injected.

Study acquisition in patients began simultaneously with the injection of the  $^{191\text{m}}\text{Ir}$  through a 17-gauge 1.5-in. Teflon intravenous needle placed in a medial antecubital fossa vein. The patient was studied in the supine position with the slant hole collimator resting closely on the chest so that a 30-degree RAO view was obtained. This view allowed a roentgenographic view equal to that obtained in contrast angiography studies, profiling the ventricle along its major axis. Data was acquired in frame mode at 2 power zoom on a  $64 \times 64$  pixel matrix at frame rates varying from 20 to 32 frames/sec for 30 sec with on-line deadtime and detector nonuniformity corrections. Data was recorded into computer memory and later to magnetic tape for archiving and data processing. Correction for the rapid radioactivity decay of  $^{191\text{m}}\text{Ir}$  was applied to all obtained data points and summarized image data.

Processing was accomplished by a nearly totally automated computer program. Data was first grouped into one second summed images over the entire period of acquisition to define the various cardiac transit phases of the bolus of activity as well as to identify the interval of time that the first pass of the bolus traversed the right and left ventricles without the appearance of overlapping structures or recirculation. The maximum one second right and left ventricular phase counts were noted. In addition, the time from the start of the acquisition to the appearance of radiotracer in the left ventricle (LV appearance time) was noted. The previously mentioned ventricular phase interval was designated to the computer's memory. By using the electrocardiogram stored with the count data to gate the cardiac cycle, the end diastolic frames in the designated ventricular phase interval were rapidly summed. This summed end diastolic frame was then normalized to maximal counts per pixel and smoothed twice by a 9-point weighted spatial smoothing program. A ventricular region of interest was then demarcated; determination of the aortic and pulmonary valve plane were made on the basis of a visual decision. Within this previously defined region of interest (ROI), an automatic edge detection program was utilized to finally detect the ventricular borders. The edge detection program employed the calculation of points of zero second derivative on each of eight radii drawn from the point of highest counts within the roughly drawn ventricular ROI. The

minimum number of counts of the points so determined was used as threshold value and limiting number for the next program step which searched point by point for the first one of the following criteria to finally determine the edge point: (a) a valley point, (b) a local second derivative threshold point, (c) an absolute minimum local threshold point found in the first detection process, or (d) the line of the original rough ventricular edge demarcation. After creating the points of the eight original radii, additional radii were drawn automatically between the original radii to find enough edge points to draw a continuous ventricular ROI. A paraventricular background ROI was then computer generated 5 pixels in width and 4 pixels distant from the ventricle. Time-activity curves were generated for both ventricular and background ROIs. The ROI counts in the end diastolic frame with maximum number of counts, as seen from the histogram, was noted for both ventricles. Background was subtracted, and corrected curves were obtained (2-4). Ejection fraction was calculated in the standard manner: total end diastolic counts minus total end systolic counts, divided by total end diastolic counts. The counts of one beat or the summation of the counts of up to 3 beats of the right ventricular phase, and 4 to 8 beats of the left ventricular phase, allowed formation of a "representative

cycle" that was compared to similar data generated by the other methods of nuclear angiography utilized in this study. Functional images utilizing end diastolic and end systolic perimeters as well as the regional ejection fraction image were also created from the "representative cycle".

Because the camera system utilized digital information, and knowing the size of the pixel matrix and acquisition magnification (zoom), distance and area on the detector surface could be translated directly to absolute measurements of maximal length and area. These maximal length and area measurements were inserted into exactly the same formula used for the calculation of left ventricular end diastolic volume by contrast technique left ventricular angiography.

#### Technetium-99m First-Pass Nuclear Angiocardigraphy Technique

In all cases,  $^{99m}\text{Tc}$  first-pass studies were performed within 5 min of the  $^{191}\text{Ir}$  studies. First-pass angiocardigraphy acquisition and processing with  $^{99m}\text{Tc}$  were carried out in exactly the same manner as that employed with  $^{191}\text{Ir}$  studies except for two major differences, injection technique and collimator. All of the patients were pre-treated with 1.75 mg of intravenous stannous chloride to allow multigated nuclear angiogra-

TABLE 1  
Iridium-191m Acquisition Data

Patient no.	BSA* sq-m <sup>†</sup>	FR <sup>‡</sup> f/s <sup>§</sup>	Dose mCi	Max-CR <sup>¶</sup> RV-kc <sup>††</sup>	Max-Cts <sup>**</sup> RV-ROI	LV-App <sup>**</sup> sec	Max-CR LV-kc	Max-Cts LV-ROI
1	1.91	20	100	290	2,547	8.10	130	1,120
2	1.84	20	160	257	2,863	9.30	188	1,765
3	1.89	20	100	280	3,374	6.50	218	1,709
4	2.10	25	160	253	3,332	9.30	166	1,431
5	1.76	20	100	281	4,209	8.25	138	1,562
6	1.77	25	110	273	2,895	8.25	210	1,875
7	1.81	20	150	259	2,507	8.30	177	1,289
8	1.82	32	150	278	3,564	5.25	163	1,559
9	1.96	20	120	267	2,536	9.85	144	1,230
10	1.81	20	100	370	4,186	9.60	201	1,930
11	1.85	25	160	247	1,073	11.80	184	1,191
12	1.86	25	150	241	2,961	9.32	191	1,633
13	1.86	20	110	230	2,913	8.25	192	3,143
14	1.93	20	110	251	3,356	8.80	163	1,552
15	1.58	20	150	246	2,305	10.20	184	1,330
16	1.84	20	110	287	2,850	8.15	135	1,220
17	1.96	20	110	259	2,396	10.10	130	1,141
18	1.85	20	110	280	3,507	8.30	184	1,422
19	1.98	25	110	255	1,795	5.20	217	1,528
20	1.77	25	150	297	2,465	11.40	113	965
Mean	1.86	22	129	270	2,882	8.71	171	1,530
s.d.	0.10	3	24	30	746	1.70	31	461

\* Body surface area.

† Square meters.

‡ Frame rate.

§ Frames per second.

¶ Maximum count rate in phase.

\*\* Counts in region of interest in "hottest" end diastolic frame.

†† Counts  $\times$  1000.

\*\* Left ventricular appearance time.

phy studies after completion of the first-pass nuclear angiography studies. Doses ranging from 18 to 25 mCi of [ $^{99m}\text{Tc}$ ] pertechnetate dissolved in <0.5 cc of normal saline solution were injected as a bolus and flushed rapidly into the vein with 20 ml of normal saline solution injected from the side arm of a three-way stopcock assembly.

In order to achieve higher counting statistics with  $^{99m}\text{Tc}$  FPNA, in 15 of the 20 total patients an ultra high efficiency, low resolution collimator (APC-1) in the 30-degree RAO view was used instead of the APC-16 collimator described previously. In five patients, it was not considered desirable to reposition the patients after a collimator change, so that the same APC-16 collimator was used for both  $^{191\text{m}}\text{Ir}$  and  $^{99m}\text{Tc}$  FPNA studies.

#### Multigated Nuclear Angiocardigraphy Technique

The multigated nuclear angiocardigraphy technique (MUGA) method of nuclear angiocardigraphy was performed in 14 of the 20 patients after previous acquisitions of

first-pass angiocardigraphy with  $^{191\text{m}}\text{Ir}$  and  $^{99m}\text{Tc}$ . It was performed in the left anterior oblique (LAO) view (45°) optimized to obtain the best separation of the two ventricles by the interventricular septum. Acquisition was performed using 2 power zoom on a  $64 \times 64$  pixel matrix at a frame time designed to give 24 frames per cardiac cycle. At least 6 million total counts were acquired in each study. An ultra high resolution, low efficiency collimator (Elscent APC-4) was employed to give better quality images since only rest MUGA studies were performed. Using this collimator, 12 to 20 min of imaging were required to complete acquisition.

After a representative left ventricular cardiac cycle was generated, a 9-point spatial smooth was performed on the images. An ROI was drawn around the left ventricle. The application of the same edge detection algorithm described in first-pass technique was used to delineate the left ventricular ROI, and a background ROI 1 pixel distant and 2 pixels in width was automatically placed around the apex of the left ventricular ROI. Count histograms were generated, the back-

**TABLE 2**  
Technetium-99m Acquisition Data

Patient no.	COLL.*	FR f/s†	Dose mCi	Max-CR‡ RV-kc	Max-Cts§ RV-ROI	LV-App¶ sec	Max-CR LV-kc	Max-Cts LV-ROI
1	APC-1	20	25	171	1,408	6.90	138	1,353
2	APC-1	20	25	132	1,614	8.40	106	805
3	APC-1	20	25	147	2,210	550	144	1,521
4	APC-1	25	25	160	1,178	9.30	148	1,350
5	APC-1	25	20	158	2,522	6.55	154	1,586
6	APC-1	25	25	146	2,546	6.05	137	1,377
7	APC-1	20	20	127	1,776	5.50	126	1,374
8	APC-1	25	20	141	2,550	5.32	117	1,980
9	APC-1	20	20	119	1,960	7.65	95	1,636
10	APC-1	20	20	142	1,650	7.00	116	1,800
11	APC-1	25	25	142	987	11.72	112	2,128
12	APC-1	25	22	145	1,707	5.70	141	1,793
13	APC-1	20	20	140	2,301	5.40	104	2,246
14	APC-1	20	20	159	3,343	5.80	133	1,476
15	APC-1	20	20	132	1,785	9.70	107	1,646
Mean	N = 15	22	22	144	1,969	7.10	125	1,604
s.d.		2	3	14	615	1.91	18	358
16	APC-16	20	23	138	1,791	5.50	93	1,132
17	APC-16	20	20	116	1,488	9.60	97	1,045
18	APC-16	20	19	124	2,028	5.80	101	818
19	APC-16	25	19	95	802	3.90	62	642
20	APC-16	25	18	101	1,480	11.50	84	925
Mean	N = 5	22	20	115	1,518	7.26	87	912
s.d.		3	2	17	461	3.16	16	192

\* Collimator.

† Frame rate.

‡ Frames per second.

§ Maximum count rate in phase.

¶ Counts in the region of interest in "hottest" end diastolic frame.

\*\* Counts  $\times$  1,000.

†† Left ventricular appearance time.

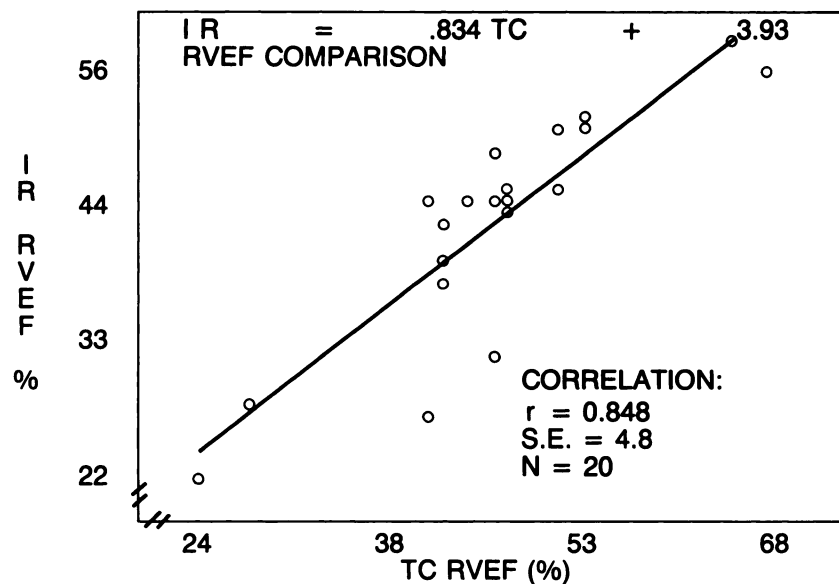


**FIGURE 1**  
Correlation of RVEF by first-pass radionuclear angiography using  $^{191}\text{Ir}$  (IR) and  $^{99\text{m}}\text{Tc}$  (TC).

ground was subtracted, and the left ventricular global ejection fraction was calculated.

#### Statistical Analysis

Tests of significant differences between the measurements of the various techniques were made by Student's *t* testing. Correlations between values obtained by all techniques were made using linear regression analysis.

## RESULTS

#### Acquisition Data

The acquisition data for  $^{191}\text{Ir}$  and  $^{99\text{m}}\text{Tc}$  FPNA nuclear angiography are shown in Table 1 and Table 2, respectively. Mean frame rates for both ventricles were equal (22 frames per second). The mean  $^{191}\text{Ir}$  dose administered was  $129 \pm 24$  mCi versus a mean

dose of  $20 \pm 2$  mCi of  $^{99\text{m}}\text{Tc}$ . In comparing the 15 patients who had  $^{99\text{m}}\text{Tc}$  FPNA with an ultra high efficiency, low resolution (APC-1) collimator with the same 15 patients who had  $^{191}\text{Ir}$  FPNA using the lower efficiency, higher resolution APC-16 collimator, the following count results were observed.

1. In all cases, the  $^{191}\text{Ir}$  FPNA maximum right ventricular count rate was markedly higher than that obtained in the  $^{99\text{m}}\text{Tc}$  FPNA study. The difference in mean values was significant ( $p < 0.001$ ).

2. In all cases the  $^{191}\text{Ir}$  FPNA maximum right ventricular ROI counts in the "hottest" end diastolic frame of the right ventricular phase was higher than that of its counterpart  $^{99\text{m}}\text{Tc}$  FPNA study. The difference in mean values was again highly significant ( $p < 0.001$ ).

3. The  $^{191}\text{Ir}$  FPNA maximum left ventricular count rate was generally considerably higher (in 13 of 15 total

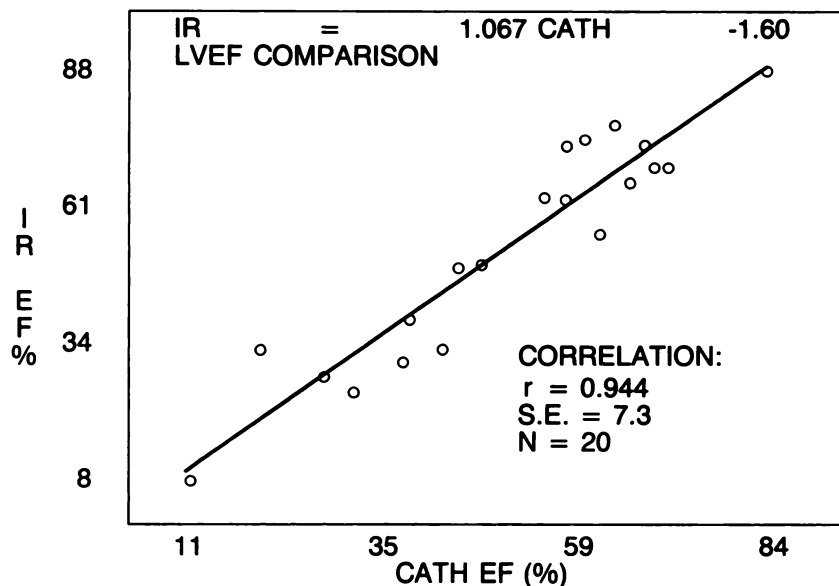


**FIGURE 2**  
Correlation of LVEF between first-pass  $^{191}\text{Ir}$  radionuclear angiography and contrast angiography performed in the cardiac catheterization laboratory.

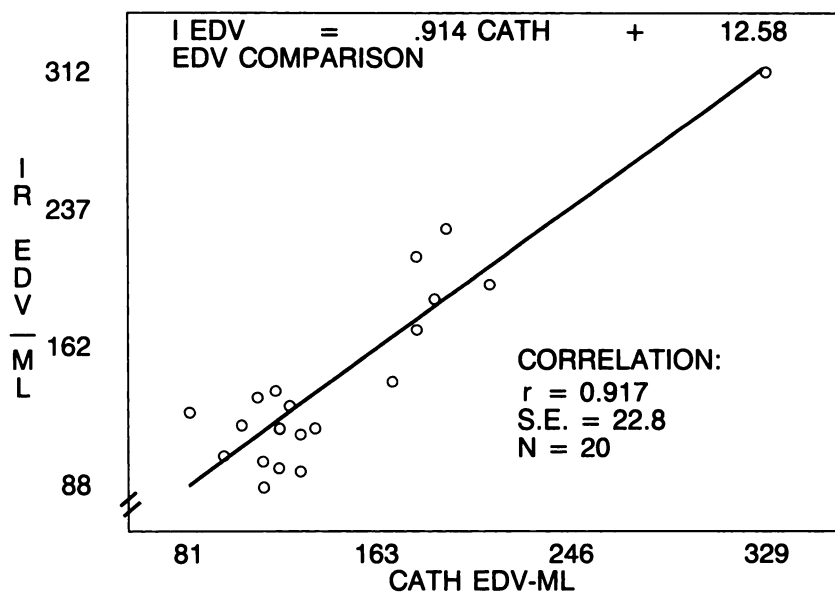


**FIGURE 3**  
 Correlation of LVEDV by first-pass  $^{191}\text{mIr}$  radionuclear angiography and contrast angiography performed in the cardiac catheterization laboratory.

comparable patients) than the value obtained in the same patient's  $^{99\text{mTc}}$  FPNA study. The difference in respective mean values was highly significant ( $p < 0.001$ ).

4. There was no significant difference between  $^{191\text{mIr}}$  and  $^{99\text{mTc}}$  FPNA studies in the counts of the left ventricular ROI in the "hottest" end diastolic frame measured in the left ventricular phase.

In the 20 total patients there was a significant difference in the interval between radiotracer injection and its initial appearance in the left ventricle. In nearly all cases the radiotracer arrived earlier to the left ventricle in the  $^{99\text{mTc}}$  FPNA study than in the counterpart  $^{191\text{mIr}}$  FPNA study. Mean values of this parameter (7.26 sec versus 8.74 sec) were significantly different ( $p < 0.001$ ). This was felt to be a result of the mechanical quality of injection. Of note, in the patients in which a power

injection from an infusion pump was used to inject  $^{191\text{mIr}}$  and its follow-up saline bolus (Patients 15 and 20) there was no appreciable difference in times.

#### Hemodynamic Parameters

The correlation between  $^{191\text{mIr}}$  studies as well as its counterpart  $^{99\text{mTc}}$  and contrast angiography studies are shown in Figures 1-4. As demonstrated, there were good correlations and relatively low standard errors of estimate when comparing  $^{191\text{mIr}}$  FPNA RVEF to  $^{99\text{mTc}}$  FPNA RVEF ( $r = 0.848$ , s.e. = 4.8) and  $^{191\text{mIr}}$  FPNA LVEF to contrast angiography LVEF ( $r = 0.944$ , s.e. = 7.3). There were no significant differences in the mean values of these parameters.

Acceptable correlation was demonstrated between  $^{191\text{mIr}}$  FPNA and contrast angiography determinations of left ventricular and diastolic volume ( $r = 0.917$ , s.e.

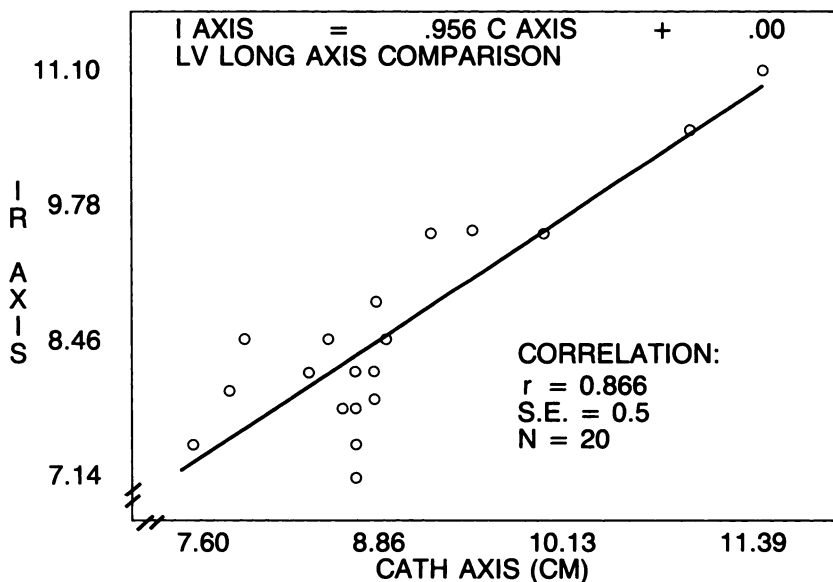


**FIGURE 4**  
 Correlation of left ventricular long axis by first pass  $^{191\text{mIr}}$  radionuclear angiography and contrast angiography performed in the cardiac catheterization laboratory.

**TABLE 3**  
**Calculated Hemodynamic Parameters**

Patient no.	RVEF (%)		LVEF (%)				EDV (ML)		AXIS (CM)	
	IR	TC	IR	TC	MU	CA	IR	CA	IR	CA
1	45	42	74	82	74	61	116	129	8.82	8.83
2	43	43	73	80		69	121	104	7.80	8.60
3	38	43	69	69	61	72	103	96	7.80	8.68
4	27	42	25	26	19	32	127	81	8.14	8.36
5	51	54	77	66	64	65	136	110	7.97	7.85
6	46	48	73	76	63	59	88	113	7.18	8.69
7	56	68	62	70	58	59	100	113	8.14	8.69
8	40	43	33	32		43	188	188	9.50	9.94
9	51	52	69	56	61	70	97	120	8.48	8.89
10	44	48	39	33	31	39	211	179	9.54	9.46
11	28	28	33	22	13	20	197	211	10.51	10.93
12	32	47	31	35		38	119	135	8.14	8.39
13	45	45	28	33		28	226	192	9.50	9.19
14	46	52	50	49	46	48	139	118	8.48	7.95
15	45	48	49	48	39	45	171	180	8.48	8.56
16	45	47	63	56	55	56	144	169	8.14	8.80
17	49	47	56	56	52	63	118	119	7.88	8.80
18	44	48	66	80		67	96	129	7.46	8.68
19	52	54	88	90		84	130	125	7.46	7.60
20	22	24	8	8	6	11	312	329	11.10	11.40
Mean	42	46	53	53	46	51	147	147	8.52	8.91
s.d.	9	9	22	23	21	19	56	56	1.03	0.93

Axis = long axis of left ventricular, CA = contrast angiography.

= 22.8) and left ventricular long axis ( $r = 0.866$ , s.e. = 0.5). Individual patient data is listed in Table 3. There were no significant differences in the mean values of these parameters.

Acceptable correlation was obtained between  $^{99m}\text{Tc}$  MUGA LVEF with contrast angiography LVEF ( $r = 0.947$ , s.e. = 7.0), although there was a significant difference ( $p < 0.001$ ) in their respective mean values (46% vs. 50%). Similarly, mean  $^{99m}\text{Tc}$  MUGA LVEF was significantly less than the mean  $^{191}\text{Ir}$  FPNA LVEF (46% vs. 53%). There was a high correlation ( $r = 0.959$ ) and no significant difference in the mean values of LVEF from the  $^{191}\text{Ir}$  FPNA and  $^{99m}\text{Tc}$  FPNA studies (53% vs. 51%).

## DISCUSSION

This study demonstrated that measurable parameters of counts, as well as the calculated parameter of global left ventricular ejection fraction, are as good in  $^{191}\text{Ir}$  FPNA studies as similar studies performed with  $^{99m}\text{Tc}$ . Certainly, the value of global LVEF obtained from  $^{191}\text{Ir}$  FPNA accurately reflected the value of global LVEF obtained by the "gold standard", contrast angiography, in this study.

The acceptable numerical correlation of LVEDV and LV long axis by  $^{191}\text{Ir}$  FPNA and contrast angiography may be somewhat misleading. Although at the high end of values little variation between the two types of methods is noted, there are considerable differences when smaller, normal, ventricular volumes or axes were compared. In these cases,  $^{191}\text{Ir}$  FPNA tended to underestimate the contrast angiography values. Thus, the importance of  $^{191}\text{Ir}$  FPNA calculated LVEDV may not be in its absolute value compared to contrast angiography, but as a baseline value to be compared after an intervention  $^{191}\text{Ir}$  FPNA study in the same patient.

In this study, no attempt was made to define reproducibility of the FPNA results due to the multiple tests performed. This shortcoming is partially tempered by the near total automation of data processing. The only observer intervention in data processing FPNA and MUGA studies occurred when an ROI was drawn to grossly demarcate an area for the edge detection analysis to begin. In all FPNA studies, this gross early observer ROI was well outside of the final computer delineated ROI. Thus, for each individual injection, no significant change would be expected in calculated count data in the edge detected ROI or in the final calculated EF. Depending on differences in bolus injection technique, there could be differences obtained by the FPNA proc-

essing. Using a power injection device as was employed in two patients of this study, would be expected to partially eliminate this problem.

Regional wall motion was not evaluated in a quantitative manner in this study. Nevertheless, the  $^{191}\text{Ir}$  FPNA left ventricular regional wall motion and functional images were found to be valuable for clinical evaluation.

First-pass nuclear angiocardigraphy with  $^{191}\text{Ir}$  may not always be useful. In patients with very prolonged transit times, most of the  $^{191}\text{Ir}$  may have decayed by the time the radiotracer reaches the cardiac chamber being examined. Although this did not happen in our study, a different method of nuclear angiocardigraphy other than  $^{191}\text{Ir}$  FPNA would need to be utilized when this occurs.

## CONCLUSIONS

Calculated count data and ventricular function data suggest that  $^{191}\text{Ir}$  FPNA performs as well as other currently accepted nuclear angiocardigraphy methods, with the advantage of a markedly lowered patient radiation dose. Its short half-life and increased photon flux allow employment of higher resolution collimators than when using  $^{99\text{m}}\text{Tc}$ . In addition,  $^{191}\text{Ir}$  FPNA would allow multiple view and multiple intervention studies in the same patient with a minimum of residual background. Thus this study supports the premise that  $^{191}\text{Ir}$ , particularly when obtained from a high specific activity and relatively long shelf-life generator, has great potential when used for first-pass nuclear angiocardigraphy.

## REFERENCES

1. Marshall RC, Berger HJ, Costin JC, et al. Assessment of cardiac performance with quantitative radionuclide angiography: sequential left ventricular ejection fraction, normalized left ventricular ejection rate, and regional wall motion. *Circulation* 1977; 56:820-829.
2. Blau F, Halama J, Lipchik E, et al. Right anterior oblique first pass radiocardiography to evaluate left ventricular ejection fraction and regional wall motion [Abstract]. *Clin Res* 1976; 26:220A.
3. Jengo JA, Mena I, Blaufuss A, et al. Evaluation of left ventricular function (ejection fraction and segmental wall motion) by single pass radioisotope angiography. *Circulation* 1978; 57:326-332.
4. Bodenheimer MN, Vanka VS, Fooshee CM, et al. Quantitative radionuclide angiography in the right anterior oblique view: comparison with contrast angiography. *Am J Cardiol* 1978; 41:718-725.
5. Rerych SK, Scholz PM, Newman GE, et al. Cardiac function at rest and during exercise in normals and in patients with coronary heart disease: evaluation by radionuclide angiocardigraphy. *Ann Surg* 1978; 187:449-463.
6. Dymond D, Stone D, Elliot AT, et al. Comparison of single plane and biplane radionuclide ventriculograms performed in oblique projections in patients with acute myocardial infarction. *Br Heart J* 1979; 42:671-679.
7. Graham TP, Goodrich JK, Robinson AE, et al. Scintiangiocardigraphy in children: rapid sequence visualization of the heart and great vessels after intravenous injection of radionuclide. *Am J Cardiol* 1970; 25:387-394.
8. Kriss JP, Enright LP, Hayden WG, et al. Radioisotope angiocardigraphy: wide scope of applicability in diagnosis and evaluation of therapy in disease of the heart and great vessels. *Circulation* 1971; 43:792-808.
9. Hurley PJ, Wesselhoeft H, James AE. Use of nuclear imaging in the evaluation of pediatric cardiac disease. *Semin Nucl Med* 1972; 2:353-372.
10. Kriss JP, Enright LP, Hayden WG, et al. Radioisotopic angiocardigraphy: findings in congenital heart disease. *J Nucl Med* 1972; 13:31-40.
11. Maltz DL, Treves S. Quantitative radionuclide angiocardigraphy: determination of Qp:Qs in children. *Circulation* 1973; 47:1049-1056.
12. Alderson PO, Jost RG, Strauss AW, et al. Radionuclide angiocardigraphy: improved diagnosis and quantification of left-to-right shunts using area ratio techniques in children. *Circulation* 1975; 51:1136-1143.
13. Cheng C, Treves S, Samuel A, et al. A new osmium-191  $\rightarrow$  iridium-191m generator. *J Nucl Med* 1980; 21:1169-1176.
14. Treves S, Kulprathipanga S, Hnatowch DJ. Angiocardigraphy with iridium-191m: an ultra short-live radionuclide (T<sub>1/2</sub> = 4.9 sec). *Circulation* 1976; 54:275-279.
15. Treves S, Cheng C, Samuel A, et al. Iridium-191m angiocardigraphy for the detection of left-to-right shunting. *J Nucl Med* 1980; 21:1151-1157.
16. Packard AB, Treves ST, O'Brien GM, et al. An osmium-191/iridium-191m radionuclide generator using an oxalato osmate parent complex. *J Nucl Med* 1987; 28:1571-1576.
17. Heller GV, Treves ST, Parker JA, et al. Comparison of ultra short-lived iridium-191m with technetium-99m for first pass radionuclide angiographic evaluation of right and left ventricular function in adults. *J Am Coll Cardiol* 1986; 7:1295-1302.
18. Issachar D, Abrashkin S, Weininger J, et al. Os-191/Ir-191m radionuclide generator based on silica-gel impregnated with tridodecylmethammonium chloride. *J Nucl Med* 1989; 30:450-457.
19. Judkins MP. Percutaneous transfemoral selective coronary arteriography. *Radiol Clin N Am* 1968; 6:467-478.
20. Kennedy JW, Trenholm SE, Kasser IS. Left ventricular volume and mass from single-plane cineangiograms: a comparison of anterior-posterior and right anterior oblique methods. *Am Heart J* 1970; 80:343-352.